Effect of Heat Treatment on Ion Conductivity of Hydrated ZrO_2 Thin Films Prepared by Reactive Sputtering Using H_2O Gas

Ning Li, Yoshio Abe, Midori Kawamura, Katsutaka Sasaki, Hidenobu Itoh, and Tsutomu Suzuki[1]

Department of Materials Science and Engineering, Kitami Institute of Technology, Kitami, Hokkaido 090-8507, Japan

[1] Department of Biotechnology and Environmental Chemistry, Kitami Institute of Technology, Kitami, Hokkaido 090-8507, Japan

Hydrated ZrO_2 thin films were prepared by reactive sputtering using H_2O gas, and these films were heat treated in air at temperatures from 100 to 350 °C. Absorbance peaks due to hydrogen-bonded OH groups for these samples were observed by Fourier transform infrared spectroscopy. The peak intensities were nearly the same before and after heat treatment below 200 °C, but began to decrease at 250 °C, and the absorption peak disappeared at 350 °C. Ion conductivity of the films was evaluated by AC impedance measurements and was found to be about 3×10^{-6} S/m before and after heat treatment at 200 °C; it also decreased after heat treatment above 250 °C. From these results, we considered that protons of OH and/or H_2O in the films are the dominant ionic species that contribute to the ion conductivity of the films.

1. Introduction

Zirconium oxide (ZrO_2) thin films have been applied in wide-ranging fields of optical and electronic industries, because ZrO_2 is a technologically important material with a high melting point (2670 °C),[1] excellent thermal stability, high refractive index, and low optical absorption in a broad wavelength region from near-UV (above 240 nm) to mid-IR (below 8 μm).[2] ZrO_2 thin films have been prepared by electron beam evaporation,[3,4] pulse laser deposition,[5] ion-assisted deposition,[6] sol-gel processing,[7-8] metal-organic chemical vapor deposition,[9] and sputtering.[10,11] In recent years, sputtering techniques have been widely used to fabricate thin films, because it is superior in its ability to form large-area films with high productivity, and it is easy to control the stoichiometry of the deposited films.[12]

Ion conductivities of hydrated ZrO_2 have been investigated, and England *et al.*[13] reported an ion conductivity of 2×10^{-5} S/cm at room temperature for $ZrO_2 \cdot 1.75H_2O$ powder prepared by a sol-gel technique. Kim *et al.*[14] reported a room-temperature ion conductivity of 1.67×10^{-6} S/cm for $ZrO_2 \cdot H_x$ thin films with x = 1.70, deposited by reactive sputtering in Ar + H_2 + O_2 atmosphere. Furthermore, ZrO_2 solid electrolyte thin films have been successfully applied to all-solid-state electrochromic devices[14-15] and switchable mirrors.[16-17] In consideration of the merits of the sputtering method and safety from the explosion of hydrogen gas, as reported in a previous paper,[18] we prepared hydrated Ta_2O_5 thin films by reactive sputtering in H_2O atmosphere. In order to confirm the feasibility of this method for the formation of other hydrated oxide films, hydrated ZrO_2 thin films were prepared in this study. We also examined the effect of heat treatment on the ion conducting characteristics of the films to confirm the proton

conduction and thermal stability of the hydrated ZrO_2 thin films.

2. Experimental Procedure

Hydrated ZrO_2 films with thicknesses of 100 nm and 1 μm were prepared by reactive RF magnetron sputtering. A 2-inch-diameter disk of the Zr target (99.9% purity) was sputtered in H_2O and D_2O gases. The sputtering gas pressure, sputtering power, and substrate temperature were maintained at 6.7 Pa, 50 W, and 10°C, respectively. These films were heat treated at temperatures from 100 to 350 °C in air atmosphere for 2 hours. Indium tin oxide (ITO)-coated glass and Si were used as substrates. Refractive index, density, crystal structure, chemical structure, and surface morphology of the deposited films were characterized by ellipsometry, X-ray reflectivity (XRR), X-ray diffraction (XRD), Fourier transform infrared spectroscopy (FTIR), and atomic force microscopy (AFM), respectively. The plasma state during sputtering was characterized by plasma emission spectroscopy. Ion conductivity was measured for the sample with the Au/ZrO_2/ITO structure shown in Fig. 1(a) by AC impedance measurements at frequencies from 10 mHz to 1 MHz at room temperature in air. The conductivity of the thin films was estimated by assuming the equivalent circuit shown in Fig. 1(b), where R_s is the resistance of the ITO electrode, R_p is the ionic resistance of the ZrO_2 film, C_d is the double-layer capacitance, and C_p is the capacitance of the ZrO_2 film. A Au film was deposited by vacuum evaporation on the ZrO_2 films as a top electrode, and ITO was used as a bottom electrode. The ZrO_2 films were removed from the sputtering chamber and kept in a desiccator before measurements.

3. Results and Discussion

Figure 2 shows the plasma emission spectra obtained during sputtering in H_2O gas. Emission peaks due to OH radicals, O_2^+ ions, H and O atoms are clearly observed.[19-20] H atoms and OH radicals are considered to be formed by the dissociation of H_2O molecules in the plasma. These active species are expected to be incorporated into the films, and hydrated ZrO_2 thin films are expected to be formed in the atmosphere of H_2O gas.

XRD patterns of the films with a thickness of 1 μm deposited on Si substrates are shown in Fig. 3, and peaks due to monoclinic-ZrO_2[21] are observed. Although these peaks are broad and weak, no other crystalline phases are found to be formed. These peaks slightly shift to a higher angle with increasing heat treatment temperature, which indicates the decrease of the lattice constant. It is known that monoclinic-ZrO_2 is formed above 650 °C,[1] however, monoclinic-ZrO_2 films were formed at a substrate temperature of 10 °C in this study. The nonequilibrium formation process by the deposition of high-energy sputtered particles is thought to be the reason for the formation of the monoclinic-ZrO_2 films.

AFM is used to study the surface topography of the films before and after heat treatment. The root mean square roughness was 2.9–3.5 nm and no marked change was observed after heat treatment up to 350 °C.

FTIR spectra of the films before and after heat treatment at different temperatures are shown in Fig. 4. As shown in Fig. 4(a), the films deposited in H_2O atmosphere have absorption peaks at approximately 740 cm^{-1} corresponding to Zr-O groups,[22,23] which indicates the formation of ZrO_2. The absorption peaks due to hydrogen-bonded OH

groups[24] are clearly seen in the region of 2800–3700 cm^{-1} for the films before and after heat treatment below 300 °C. The peak intensity decreases slightly at 250°C, and disappears completely at 350 °C. Figure 4(b) shows FTIR spectra of the films prepared in D_2O atmosphere. The wave-number region is changed to 1000–7000 cm^{-1} in this figure to clearly indicate the OH and OD peaks and the influence of interference. The absorption peaks due to hydrogen-bonded OD groups[25] are observed in the region of 2000–2600 cm^{-1}. This clearly indicates that water molecules were introduced into the film during the reactive sputtering process. However, the intensity of the absorption peaks due to OD groups decreased gradually, and the peaks due to OH groups increased when the films were kept in air. It is thought that the exchange of D_2O molecules in the film and H_2O molecules in air progresses even at room temperature. With increasing heat treatment temperature, the absorption peaks due to OD groups decreased greatly. The absorption peaks due to OH groups increased abruptly after heat treatment at 100 °C and then decreased slightly with the increase of heat treatment temperature. The increase in the intensity of the peak due to OH groups indicates that a large part of OH and/or H_2O in the films originate from H_2O molecules in ambient atmosphere.

We estimated the molar concentration of water in the films using Lambert-Beer's law,

$$A = \log\left(\frac{1}{T}\right) = \varepsilon c d \,, \tag{1}$$

where A, T, ε, c, and d represent the absorbance, transmittance, molar absorption coefficient, molar concentration of the medium, and thickness, respectively. The molar absorption coefficient of water in the films was assumed to be the same as that of pure water, ε = 93.7 l/ (mol·cm), which is calculated from

 , (2)

where k and λ are the extinction coefficient of water (0.2804 at 3404 cm^{-1})[26] and wavelength, respectively. The molar concentration of pure water is 55.5 mol/ l.

Film density estimated from the XRR measurement is shown in Fig. 5. The film density becomes higher with increasing heat treatment temperature, however, it is still lower than the bulk value of 5.85 g/cm^3 for monoclinic-ZrO_2.[1] Figure 6 shows the change in the refractive index after heat treatment measured with an ellipsometer at a wavelength of 633 nm. The refractive index increases from 1.90 to 1.92 with the increase of heat treatment temperature, and the values are small compared with the value of 2.15 for bulk monoclinic-ZrO_2.[1] The low refractive index corresponds to the low film density.

From the results above, it is thought that the low film density of the ZrO_2 films is due to the introduction of H_2O molecules into and/or between ZrO_2 grains and the porous structure of the film. Therefore, we assumed the film density ρ_{film} to be given by

$$\rho_{film} = q_{ZrO_2}\rho_{ZrO2} + q_{H_2O}\rho_{H_2O} + q_{void}\rho_{void}, \quad (3)$$

where ρ_{ZrO_2} is the density of bulk monoclinic-ZrO_2 (5.85 g/cm^3) and ρ_{H_2O} is the density of water (0.997 g/cm^3 at 25 °C), and q_{ZrO_2}, q_{H_2O}, and q_{void} are the volume fractions of bulk ZrO_2, H_2O, and voids, respectively. q_{H_2O} is calculated from eq. (1). The density of voids ρ_{void} is ignored ($\rho_{void} = 0$), and the sum of the volume fractions is assumed to be unity ($q_{ZrO_2} + q_{H_2O} + q_{void} = 1$). The refractive index of the film n_{film} is

also assumed to be given by the following equation (Drude theory):[27)]

$$n_{film}{}^2 - 1 = q_{ZrO_2}\left(n_{ZrO_2}{}^2 - 1\right) + q_{H_2O}\left(n_{H_2O}{}^2 - 1\right) + q_{void}\left(n_{void}{}^2 - 1\right), \quad (4)$$

where n_{ZrO_2}, n_{H_2O}, and n_{void} represent refractive indexes of ZrO_2, H_2O, and voids, respectively. The values of n_{ZrO_2}, n_{H_2O}, and n_{void} are assumed to be 2.15, 1.33, and 0, respectively. The results of the volume fractions are shown in Fig. 7. Although the volume fractions calculated from the density and refractive index differ slightly, it is clearly seen that the volume fractions of monoclinic-ZrO_2 and void increase slightly with increasing heat treatment temperature owing to the loss of H_2O molecules. From the volume fractions of ZrO_2 and H_2O, molar ratio n of H_2O in the $ZrO_2 \cdot nH_2O$ film was estimated to be approximately 0.2 for the as-deposited film.

Cole-Cole plots of complex impedance (R and X are the real and imaginary parts of complex impedance, respectively) are shown in Fig. 8. The resistances R_p due to ion conduction are obtained from the diameters of the semicircles in the Cole-Cole plots. [28)] The resistances of the films before and after heat treatment at 100–200 °C were in the order of 10^4 Ω; however, they began to increase after heat treatment at 250 °C. The ionic conductivity of the films σ_i was calculated using

$$\sigma_i = \frac{d}{R_p S}, \quad (5)$$

where d, R_p, and S are the film thickness, the film resistance estimated from the Cole-Cole plots, and the area of the electrodes, respectively. Figure 9 shows the change in the ion conductivity of the films before and after heat treatment. High ion conductivity of 3×10^{-6} S/m was obtained for the as-deposited ZrO_2 films. The lower conductivity compared with those of $ZrO_2 \cdot 1.75H_2O$ powders[13)] and $ZrO_2 \cdot H_{1.70}$ thin

films[14] are thought to be caused by the lower H_2O content in our films, as described above. The ion conductivity was maintained high even after heat treatment at 200 °C, however, it began to decrease after heat treatment above 250 °C. Even though some of H_2O molecules are desorbed from the film during heat treatment, H_2O molecules are absorbed by the films again at room temperature, owing to the low film density and porous structure of the ZrO_2 films. This result indicates that protons in the hydrated ZrO_2 films contribute to the ion conduction. The ion conductivity of the ZrO_2 films is similar to that (4×10^{-6} S/m) of the Ta_2O_5 films reported in our previous paper,[18] and the ion conductivity of the ZrO_2 films remains high after heat treatment at higher temperatures than that of the Ta_2O_5 films. These results suggest that the hydrated ZrO_2 films are a promising candidate for solid electrolyte thin films.

4. Conclusions

Hydrated ZrO_2 thin films were fabricated by reactive sputtering using H_2O gas, and ion conductivity of 3×10^{-6} S/m was obtained for the as-deposited film. It was indicated that protons in the hydrated ZrO_2 films contribute to the ion conduction, and the ion conductivity was confirmed to be stable after heat treatment up to 200 °C. Because of these results, the hydrated ZrO_2 film is considered to be a promising candidate for proton-conducting solid electrolyte thin films.

References

1) K. Tanabe, T. Seiyama, and K. Fueki: *Kinzoku Sankabutsu to Fukugo Sankabutsu* (Metal Oxides and Composite Oxides) (Kodansha, Tokyo, 1978) p. 119 [in Japanese].

2) H. K. Pulker: *Coatings on Glass* (Elsevier, Amsterdam, 1999) p. 410.

3) M. G. Krishna, K. N. Rao, and S. Mohan: Thin Solid Films **193-194** (1990) 690.

4) S. Shao, Z. Fan, J. Shao, and H. He: Thin Solid Films **445** (2003) 59.

5) A. Husmann, J. Gottmann, T. Klotzbücher, and E. W. Kreutz: Surf. Coat. Technol. **100-101** (1998) 411.

6) M. G. Krishna, K. N. Rao, and S. Mohan: Thin Solid Films **207** (1992) 248.

7) A. Mehner, H. Klümper-Westkamp, F. Hoffmann, and P. Mayr: Thin Solid Films **308-309** (1997) 363.

8) R. Brenier, C. Urlacher, J. Mugnier, and M. Brunel: Thin Solid Films **338** (1999) 136.

9) J. S. Kim, H. A. Marzouk, and P. J. Reucroft: Thin Solid Films **254** (1995) 33.

10) N. Iwamoto, Y. Makino, and M. Kamai: Thin Solid Films **153** (1987) 233.

11) M. Boulouz, A. Boulouz, A. Giani, and A. Boyer: Thin Solid Films **323** (1998) 85.

12) K. P. S. S. Hembram, G. Dutta, U. V. Waghmare, and G. M. Rao: Physica B **339** (2007) 21.

13) W. A. England, M. G. Cross, A. Hamnett, P. J. Wiseman, and J. B. Goodenough: Solid State Ionics **1** (1980) 231.

14) S. H. Kim, J. H. Ko, S. H. Ji, J. S. Kim, S. S. Kang, M.-J. Lee, and Y. S. Yoon: Jpn. J. Appl. Phys. **45** (2006) 5144.

15) A.-L. Larsson and G. A. Niklasson: Sol. Energy Mater. Sol. Cells **84** (2004) 351.

16) V. M. M. Mercier and P. van der Sluis: Solid State Ionics **145** (2001) 17.

17) R. Armitage, M. Rubin, T. Richardson, N. O'Brien, and Y. Chen: Appl. Phys. Lett. **75** (1999) 1863.

18) Y. Abe, F. Peng, Y. Takiguchi, M. Kawamura, K. Sasaki, H. Itoh, and T. Suzuki: Jpn. J. Appl. Phys. **47** (2008) 7269.

19) D. R. Lide: *CRC Handbook of Chemistry and Physics* (CRC Press, Boca Raton, FL, 2003) 84th ed., Sect. 10.

20) R. W. B. Pearse and A. G. Gaydon: *The Identification of Molecular Spectra* (Chapman and Hall, London, 1976) p. 261.

21) International Center for Diffraction Data (ICDD), Powder Diffraction File (PDF)-2, Release 2009, reference code 00-037-1484.

22) G. Štefanić, S. Musić, and A. Gajović: J. Mol. Struct. **744-747** (2005) 541.

23) I. I. Štefanć, S. Musić, G. Štefanić, and A. Gajović: J. Mol. Struct. **480-481** (1999) 621.

24) Y. Sone, A. Kishimoto, and T. Kudo: Solid State Ionics **66** (1993) 53.

25) M. Takeuchi and M. Anpo: Materials Integration **19** (2006) 35 [in Japanese].

26) M. R. Querry, D. M. Wieliczka, and D. J. Seselsteim: in *Handbook of Optical Constants of Solids Ⅱ*, ed. E. D. Palik (Academic Press, San Diego, CA, 1991) p. 1059.

27) R. Jacobsson: in *Physics of Thin Films* ed. G. Hass, M. H. Francombe, and R. W. Hoffman (Academic Press, New York, 1975) Vol. 8, p. 51.

28) T. Osaka, N. Oyama, and T. Ohsaka: *Denki Kagaku Ho – Kiso Sokutei Manual* (Electrochemical Method – Manual of Fundamental Measurement) (Kodansha, Tokyo,

2002) p. 94 [in Japanese].

Figure captions

Fig.1. Structure of samples used for impedance measurement (a) and assumed equivalent circuit for the evaluation of ionic conductivity of the film (b).

Fig. 2. Plasma emission spectrum during sputtering in H_2O atmosphere.

Fig. 3. XRD patterns of hydrated ZrO_2 thin films with a thickness of 1 μm before and after heat treatments at different temperatures.

Fig. 4. FTIR spectra of hydrated ZrO_2 thin films deposited in H_2O atmosphere (a) and in D_2O atmosphere (b) to a thickness of 1 μm before and after heat treatment at different temperatures.

Fig. 5. Density of hydrated ZrO_2 thin films as a function of heat treatment temperature. The density was estimated from XRR measurement results for sample with a thickness of 100 nm.

Fig. 6. Refractive index of hydrated ZrO_2 thin films as a function of heat treatment temperature. The refractive index was measured by ellipsometry at a wavelength of 633 nm for samples with a thickness of 100 nm.

Fig. 7. Volume fractions of monoclinic-ZrO_2 (diamonds), H_2O (circles), and voids (squares) as functions of heat treatment temperature. Solid lines and filled marks were values estimated from eq. (3) and dotted lines and open marks were those estimated from eq. (4).

Fig. 8. Cole-Cole plots of hydrated ZrO_2 thin films with a thickness of 1 μm before and after heat treatment at different temperatures.

Fig. 9. Ion conductivity of hydrated ZrO_2 thin films as a function of heat treatment

temperature.

Fig. 1

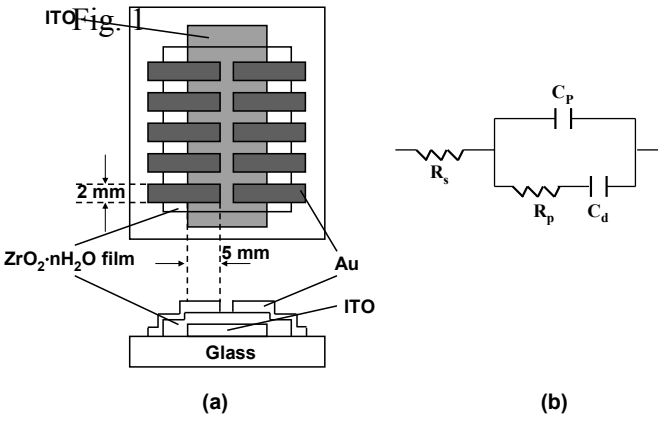

Fig. 2

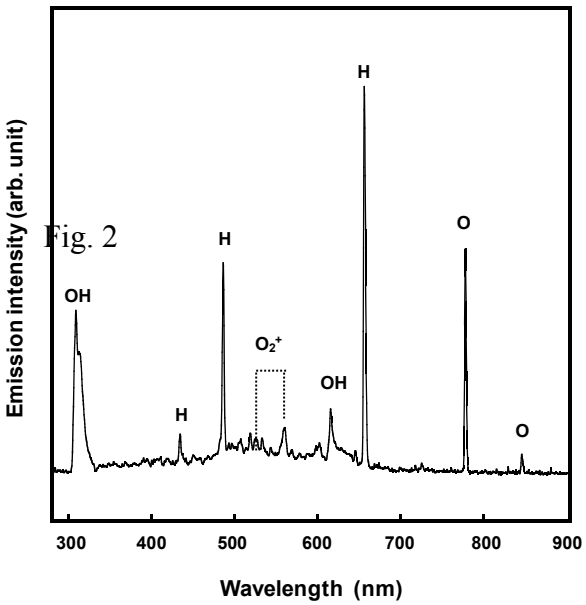
Emission intensity (arb. unit)
OH
H
H
O_2^+
OH
H
O
O
300
400
500
600
700
800
900
Wavelength (nm)

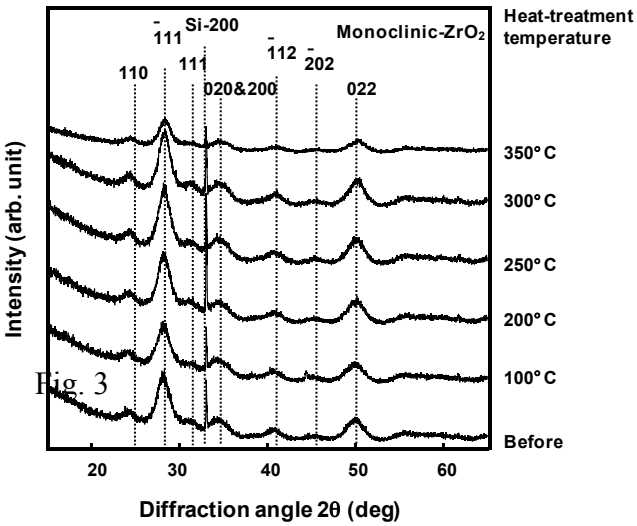
Heat-treatment temperature
Monoclinic-ZrO2
Si-200
-111
111
110
-112
-202
020&200
022
350° C
300° C
250° C
200° C
100° C
Before
Intensity (arb. unit)
20
30
40
50
60
Diffraction angle 2θ (deg)

Fig. 3

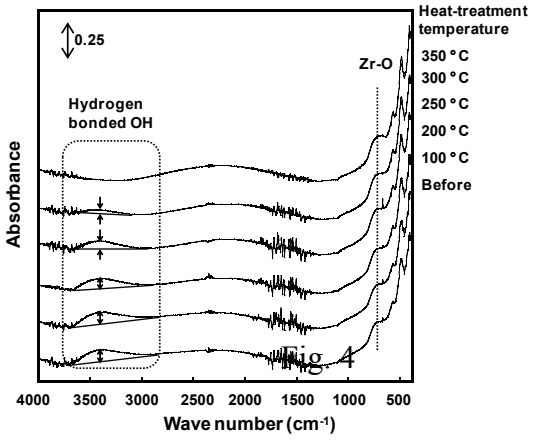
0.25
Zr-O
Hydrogen
bonded OH
Heat-treatment
temperature
350 °C
300 °C
250 °C
200 °C
100 °C
Before
Absorbance
4000 3500 3000 2500 2000 1500 1000 500
Wave number (cm-1)

(a)

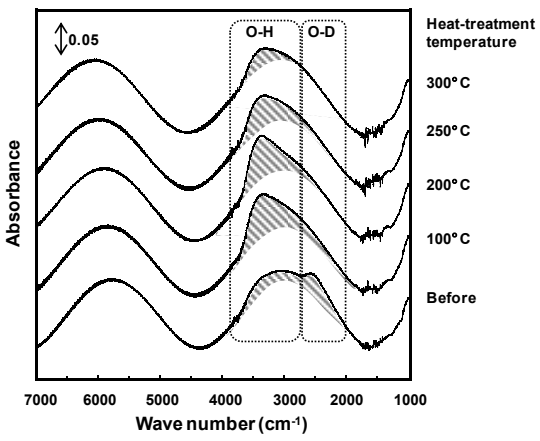
0.05
O-H
O-D
Heat-treatment
temperature
300°C
250°C
200°C
100°C
Before
Absorbance
7000 6000 5000 4000 3000 2000 1000
Wave number (cm-1)

(b)

Fig. 4

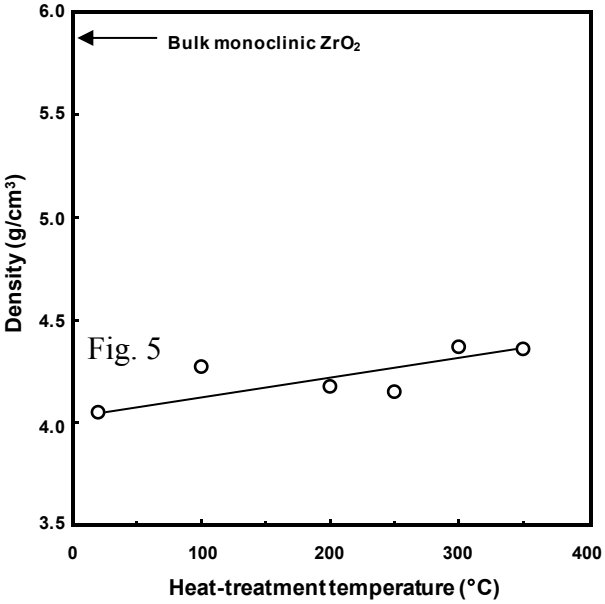
Bulk monoclinic ZrO_2
Density (g/cm³)
6.0
5.5
5.0
4.5
4.0
3.5
0
100
200
300
400
Heat-treatment temperature (°C)

Fig. 5

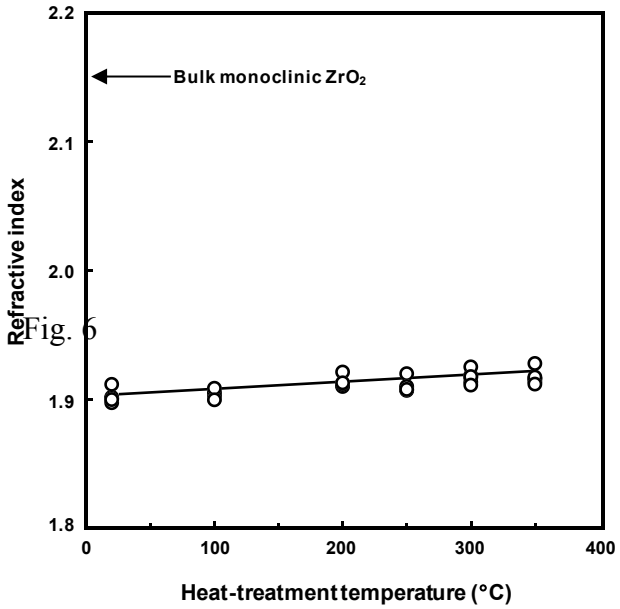
Bulk monoclinic ZrO_2
Refractive index
2.2
2.1
2.0
1.9
1.8
0
100
200
300
400
Heat-treatment temperature (°C)

Fig. 6

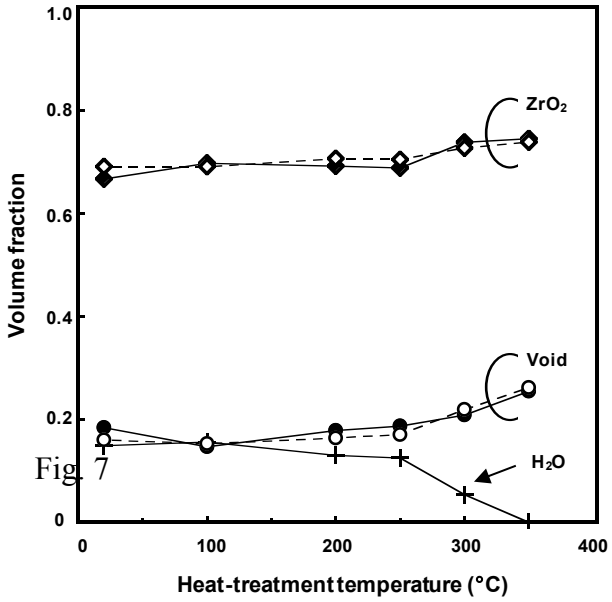
1.0
0.8
0.6
0.4
0.2
0
Volume fraction
ZrO2
Void
H2O
0
100
200
300
400
Heat-treatment temperature (°C)

Fig. 7

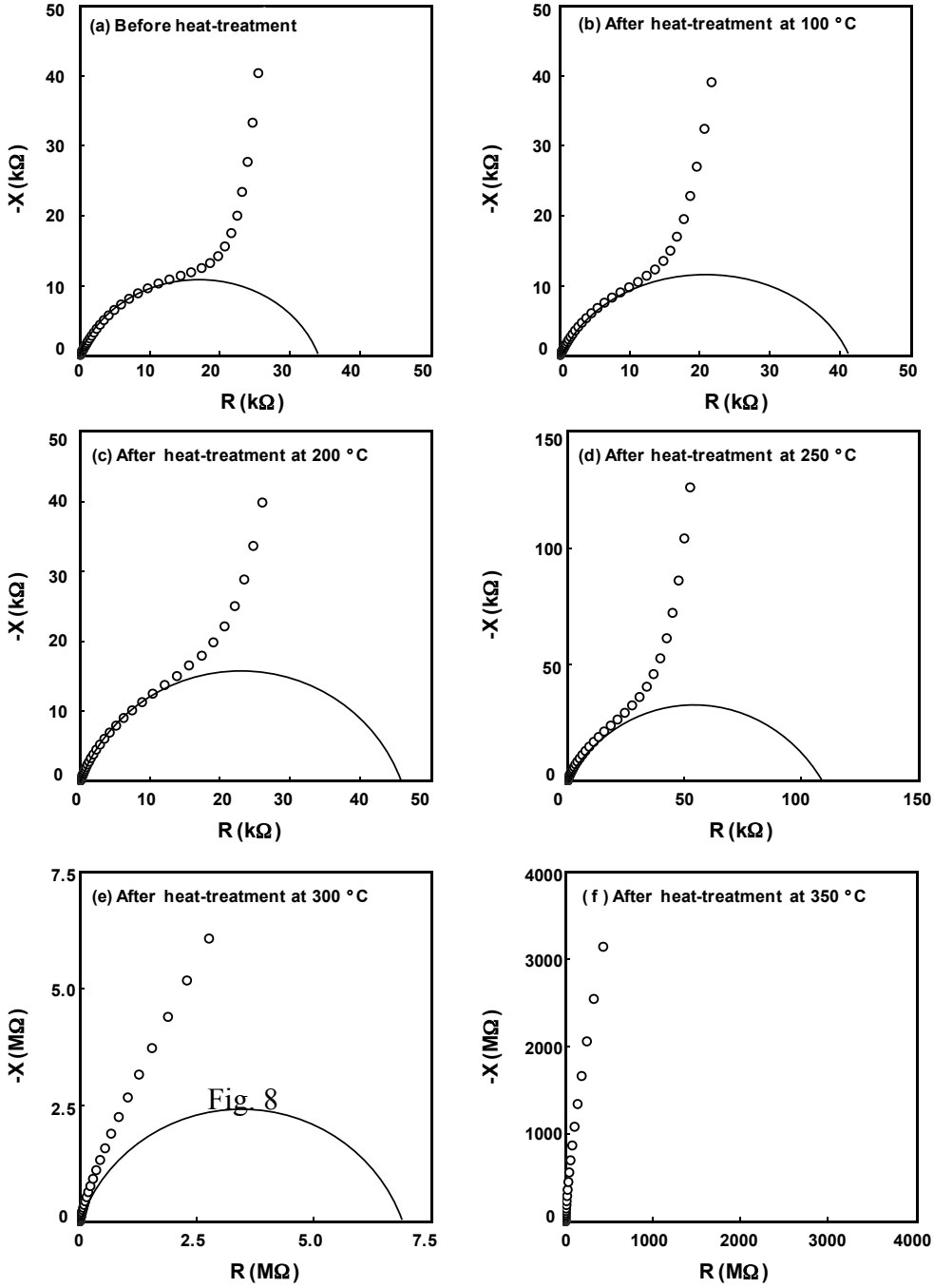
(a) Before heat-treatment
(b) After heat-treatment at 100 °C
(c) After heat-treatment at 200 °C
(d) After heat-treatment at 250 °C
(e) After heat-treatment at 300 °C
(f) After heat-treatment at 350 °C
-X (kΩ)
-X (MΩ)
R (kΩ)
R (MΩ)

Fig. 8

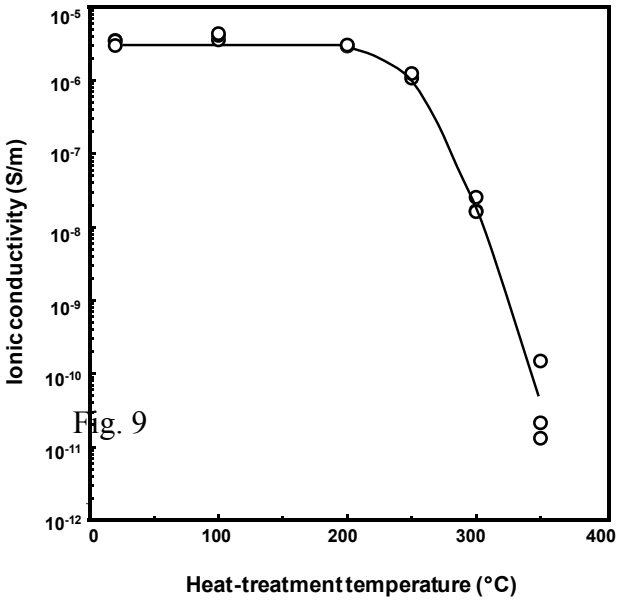
Ionic conductivity (S/m)
10-5
10-6
10-7
10-8
10-9
10-10
10-11
10-12
0
100
200
300
400
Heat-treatment temperature (°C)

Fig. 9